

CAT: LoCalization and IdentificAtion Cascade Detection Transformer for Open-World Object Detection

Shuailei Ma^{1*} Yuefeng Wang^{1†} Jiaqi Fan¹ Ying Wei^{1‡}

Thomas H. Li³ Hongli Liu² Fanbing Lv²

¹Northeast University, ²Changsha Hisense Intelligent System Research Institute Co., Ltd.

³Information Technology R&D Innovation Center of Peking University,

Abstract

Open-world object detection (OWOD), as a more general and challenging goal, requires the model trained from data on known objects to detect both known and unknown objects and incrementally learn to identify these unknown objects. The existing works which employ standard detection framework and fixed pseudo-labelling mechanism (PLM) have the following problems: (i) The inclusion of detecting unknown objects substantially reduces the model’s ability to detect known ones. (ii) The PLM does not adequately utilize the priori knowledge of inputs. (iii) The fixed selection manner of PLM cannot guarantee that the model is trained in the right direction. We observe that humans subconsciously prefer to focus on all foreground objects and then identify each one in detail, rather than localize and identify a single object simultaneously, for alleviating the confusion. This motivates us to propose a novel solution called CAT: LoCalization and IdentificAtion Cascade Detection Transformer which decouples the detection process via the shared decoder in the cascade decoding way. In the meanwhile, we propose the self-adaptive pseudo-labelling mechanism which combines the model-driven with input-driven PLM and self-adaptively generates robust pseudo-labels for unknown objects, significantly improving the ability of CAT to retrieve unknown objects. Comprehensive experiments on two benchmark datasets, i.e., MS-COCO and PASCAL VOC, show that our model outperforms the state-of-the-art in terms of all metrics in the task of OWOD, incremental object detection (IOD) and open-set detection.

1. Introduction

Open-world object detection (OWOD) is a more practical detection problem in computer vision, making arti-



Figure 1. When faced with new scenes in open world, humans subconsciously focus on all foreground objects and then identify them in detail in order to alleviate the confusion between the known and unknown objects and get a clear view. Motivated by this, our CAT utilizes the shared decoder to decouple the localization and identification process in the cascade decoding way, where the former decoding process is used for localization and the latter for identification.

cial intelligence (AI) smarter to face more difficulties in real scenes. Within the OWOD paradigm, the model’s life-span is pushed by iterative learning process. At each episode, the model trained only by known objects needs to detect known objects while simultaneously localizing unknown objects and identifying them into the unknown class. Human annotators then label a few of these tagged unknown classes of interest gradually. The model given these newly-added annotations will continue to incrementally update its knowledge without retraining from scratch.

Recently, the work [17] proposed an open-world object detector, ORE, based on the two-stage Faster R-CNN [33] pipeline. ORE utilizes an auto-labelling step to obtain pseudo-unknowns for training model to detect unknown objects and learns an energy-based binary classifier to distinguish the unknown class from known classes. However, its success largely relies on a held-out validation set which

*First author. Email: xiaomabufei@gmail.com

†Code url: <https://github.com/xiaomabufei/CAT>

‡Corresponding author. Email: weiyi@ise.neu.edu.cn

is leveraged to estimate the distribution of unknown objects in the energy-based classifier. To alleviate the problems in ORE, OW-DETR [13] proposes to use the detection transformer [3, 38] for OWOD in a justifiable way and directly leverages the framework of DDETR [38]. In addition, OW-DETR proposes an attention-driven PLM which selects pseudo labels for unknown objects according to the attention scores.

For the existing works, we find the following hindering problems. (i) Owing to the inclusion of detecting unknown objects, the model’s ability to detect known objects substantially drops. To alleviate the confusion between known and unknown objects, humans prefer to dismantle the process of open-world object detection rather than parallelly localize and identify open-world objects like most standard detection models. (ii) To the best of our knowledge, in the existing OWOD PLM, models leverage the learning process for known objects to guide the generation of pseudo labels for unknown objects, without leveraging the prior conditions of the inputs (*texture, light flow, etc*). As a result, the model cannot learn knowledge beyond the data annotation. (iii) The fixed selection manner of PLM cannot guarantee that the model learns to detect unknown objects in the right direction, due to the uncertain quality of the pseudo labels. The models may be worse for detecting unknown objects.

When faced with a new scene, humans prefer focusing on all foreground objects and then analyse them in detail, as shown in Figure.1. Motivated by this and the aforementioned observations, we propose a novel LoCalization and Identification Cascade Detection Transformer. CAT comprises three dedicated components namely, **self-adaptive pseudo-labelling mechanism**, **shared transformer decoder** and **cascade decoupled decoding structure**. The self-adaptive PLM maintains the ability of CAT to explore the knowledge beyond the known objects and self-adaptively adjusts the pseudo-label generation according to the model training process. Via the cascade decoupled decoding structure, the shared transformer decoder decouples the localization and identification process for alleviating the influence of detecting unknown objects on the detection of known objects, where the former decoding process is used for localization and the latter for identification. In the meanwhile, we observe the structure substantially improves the model’s ability for incremental object detection according to the experiments. In addition, we explore the decoupled structures for detection transformer. Our contributions can be summarized fourfold:

- We propose a novel localization and identification cascade detection transformer (CAT), which decouples the localization and identification process of detection and alleviates the influence of detecting unknown objects on the detection of known ones.
- We introduce a novel pseudo-labelling mechanism

which self-adaptively combines the model-driven and input-driven pseudo-labelling during the training process for generating robust pseudo-labels and exploring knowledge beyond known objects.

- We explore the decoupled decoding methods of the detection transformer, *i.e.*, the fully decoupled decoding structure and the cascade decoupled decoding structure.
- Our extensive experiments on two popular benchmarks demonstrate the effectiveness of the proposed CAT. CAT outperforms the recently introduced ORE and OW-DETR for OWOD, IOD and open-set detection. For OWOD, CAT achieves absolute gains ranging from **11.8%** to **18.3%** in terms of unknown recall over OW-DETR.

2. Problem Formulation

At time t , let $\mathcal{K}^t = \{1, 2, \dots, C\}$ denote the set of known object classes and $\mathcal{U}^t = \{C + 1, \dots\}$ denote the unknown classes which might be encountered at the test time. The known object categories \mathcal{K}^t are labeled in the dataset $\mathcal{D}^t = \{\mathcal{J}^t, \mathcal{L}^t\}$ where \mathcal{J}^t denotes the input images and \mathcal{L}^t denotes the corresponding labels at time t . The training image set consists of M images $\mathcal{J}^t = \{i_1, i_2, \dots, i_M\}$ and corresponding labels $\mathcal{L}^t = \{\ell_1, \ell_2, \dots, \ell_M\}$. Each $\ell_i = \{\mathcal{T}_1, \mathcal{T}_2, \dots, \mathcal{T}_N\}$ denotes a set of N object instances with their class labels $c_n \in \mathcal{K}^t$ and locations, x_n, y_n, w_n, h_n denote the bounding box center coordinates, width and height respectively. The Open-World Object Detection removes the artificial assumptions and restrictions in traditional object detection and makes object detection tasks more aligned with real life. It requires the trained model \mathcal{M}_t not only to detect the previously encountered known classes C but also to identify an unseen class instance as belonging to the unknown class. In addition, it requires the object detector to be capable of incremental update for new knowledge and this cycle continues over the detector’s lifespan. In incremental updating phase, the unknown instances identified by \mathcal{M}_t are annotated manually, and along with their corresponding training examples, update \mathcal{D}^t to \mathcal{D}^{t+1} and \mathcal{K}^t to $\mathcal{K}^{t+1} = \{1, 2, \dots, C, \dots, C + n\}$, the model adds the n new classes to known classes and updates itself to \mathcal{M}_{t+1} without retraining from scratch on the whole dataset \mathcal{D}^{t+1} .

3. Proposed method

This section elaborates the proposed CAT in details. In Sec.3.1, the overall architecture of CAT is described in detail. A novel self-adaptive adjustment strategy for pseudo-labelling is proposed in Sec.3.2. We explore to decouple the decoding process of the detection transformer and propose the localization and identification cascade decoupled

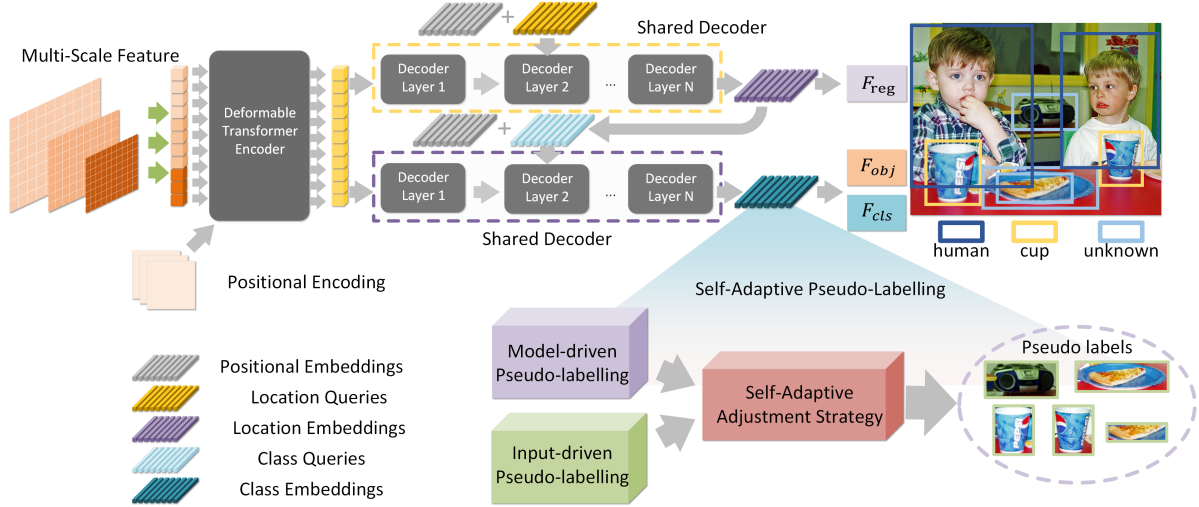


Figure 2. Overall Architecture of proposed CAT framework. The proposed CAT consists of a multi-scale feature extractor, the shared transformer decoder, the regression prediction branch, and the self-adaptive pseudo-labelling. The multi-scale feature extractor comprises the mainstream feature extraction backbone and a deformable transformer encoder, for extracting multi-scale features. The shared transformer decoder is a deformable transformer decoder and decouples the localization and identification process in the cascade decoding way. The regression prediction branch contains the bounding box regression branch F_{reg} , novelty objectness branch F_{obj} , and novelty classification branch F_{cls} . While the novelty classification and objectness branches are single-layer feed-forward networks (FFN) and the regression branch is a 3-layer FFN.

decoding structure in Sec.3.3. In Sec.3.4, we illustrate the end-to-end training strategy of CAT.

3.1. Overall Architecture

As shown in Figure.2, for a given image $\mathcal{I} \in \mathbb{R}^{H \times W \times 3}$, CAT uses a hierarchical feature extraction backbone to extract multi-scale features $Z_i \in \mathbb{R}^{\frac{H}{4 \times i^2} \times \frac{W}{4 \times i^2} \times 2^i C_s}$, $i = 1, 2, 3$. The feature maps Z_i are projected from dimension C_s to dimension C_d by using 1×1 convolution and concatenated to N_s vectors with C_d dimensions after flattening out. Afterwards, along with supplement positional encoding $P_n \in \mathbb{R}^{N_s \times C_d}$, the multi-scale features are sent into the deformable transformer encoder to encode semantic features. The encoded semantic features $M \in \mathbb{R}^{N_s \times C_d}$ are acquired and sent into the shared decoder together with a set of N learnable location queries and positional embeddings $P_m \in \mathbb{R}^{N_s \times C_d}$. Aided by interleaved cross-attention and self-attention modules, the shared decoder transforms the location queries $Q_{location} \in \mathbb{R}^{N \times D}$ to a set of N location query embeddings $\mathcal{E}_{location} \in \mathbb{R}^{N \times D}$. The $\mathcal{E}_{location}$ are then input to the regression branch to locate N foreground bounding boxes containing the known classes and unknown classes. Meanwhile, the $\mathcal{E}_{location}$ are used as class queries and sent into the shared decoder together with the M and P_m again. The shared decoder transforms the class queries to N class query embeddings \mathcal{E}_{class} that are corresponding to the location query embeddings. The \mathcal{E}_{class} are then sent into the objectness and novelty classification branch to predict

the objectness and category respectively. After selecting the unique queries that best match the known instances by a bipartite matching loss, the remaining queries are utilized to select the unknown category instances and generate pseudo labels by self-adaptive pseudo-labelling mechanism.

3.2. Self-Adaptive Pseudo-labelling

Pseudo labels play an important role in guiding models to detect unknown object instances, determining the upper learning limitation of the model. The existing methods [13, 17] only use model-driven pseudo-labelling and do not take full advantage of the inputs' priori knowledge (light flow, textures, etc). The model-driven pseudo-labelling [13] makes the model's learning get caught up in the knowledge of known objects, for the reason that the only source of knowledge for the model is known object instances. In addition, their fixed selection manner cannot guarantee the right learning direction for unknown objects. We propose to combine model-driven with input-driven pseudo-labelling [31, 36, 39] for expanding the knowledge sources of the model. In the meanwhile, the pseudo-labels selection scheme should not be fixed, but be adapted as training and able to adjust itself when facing the unexpected problems. In this paper, a novel pseudo-labelling mechanism is proposed for self-adaptively combining model-driven and input-driven pseudo-labelling according to the situation faced by the model, where the attention-driven pseudo-labelling [13] is used as the model-driven pseudo-

labelling and selective search [36] is selected as the input-driven pseudo-labelling. In self-adaptive pseudo-labelling mechanism, the model-driven pseudo-labelling generates pseudo-labels' candidate boxes P^m and the corresponding confidence s_o , and the input-driven pseudo-labelling generates pseudo-label candidate boxes P^I . The object confidence of generated pseudo labels is formulated as follows:

$$S_i = (\text{norm}(s_o))^{\mathcal{W}_m} \cdot \left(\max_{1 \leq j \leq |P^I|} \left(\text{IOU}(P_j^I, P_i^m) \right) \right)^{\mathcal{W}_I}, \quad (1)$$

where $\text{IOU}(\cdot)$ (Intersection-over-union [34]) is the most commonly used metric for comparing the similarity between two arbitrary shapes, i denotes the index of the pseudo labels. \mathcal{W}_m and \mathcal{W}_I are the self-adaptive weights, which are controlled by the *Measurer*, *Sensor* and *Adjuster*, as formulated below:

$$\mathcal{W}^t = \text{Adjuster}(\mathcal{W}^{t-1}, \text{Sensor}(\text{Measurer}(L_m))), \quad (2)$$

where L_m represents the loss memory which is stored and updated in real time during model training. The formulation is illustrated in Equation.3:

$$L_m = \text{DEQUE}(\text{loss}_{t-1}, \text{loss}_{t-2}, \dots, \text{loss}_{t-n}), \quad (3)$$

where t is the current iteration. Considering the sensitivity of the model and the uneven quality of the data, we leverage *Measurer* to obtain the trend of the losses Δl for replacing the single loss. The formula is as follows:

$$\text{Measurer}(L_m) = \frac{\sum_{i=1}^n \alpha_i \cdot \text{loss}_{t-i}}{\sum_{j=n+1}^N \beta_j \cdot \text{loss}_{t-j}}, \quad n < N < T, \quad (4)$$

where α and β denote the weighted average weights and $\sum_{i=1}^n \alpha_i = \sum_{j=n+1}^N \beta_j = \frac{\alpha_i - \alpha_{i-1}}{\alpha_{i+1} - \alpha_i} = \frac{\beta_j - \beta_{j-1}}{\beta_{j+1} - \beta_j} = 1$. In the *Sensor*, the variable of the weight Δw is acquired as follows:

$$\text{Sensor}(\Delta l) = \begin{cases} \pi_{nma} \cdot \text{Sigmoid}(\Delta l - 1), & \Delta l > 1, \\ -\pi_{pma} \cdot \Delta l, & \Delta l \leq 1, \end{cases} \quad (5)$$

where π_{pma} and π_{nma} represents the positive and negative momentum amplitude, respectively. In the *Adjuster*, we use Equation.6 to update the self-adaptive weight via an incremental way [5, 14, 17], for memory storage and enhancing the robustness (more explanations in Appendix A.1).

$$\begin{cases} \mathcal{W}_m^t = \mathcal{W}_m^{t-1} + \Delta w \times \mathcal{W}_m^{t-1}, \\ \mathcal{W}_I^t = \mathcal{W}_I^{t-1} - \Delta w \times \mathcal{W}_I^{t-1}, \\ \mathcal{W}_m^t, \mathcal{W}_I^t = \text{norm}(\mathcal{W}_m^t, \mathcal{W}_I^t), \end{cases} \quad (6)$$

where $\text{norm}(\cdot)$ is the normalization operation. The update strategy for the weights during training is shown in Algorithm.1.

Algorithm 1 COMPUTINGADAPTIVEWEIGHTS

Input: Loss Memory: L_m ; Current Iteration: t ; Positive Momentum Amplitude: π_{pma} ; Negative Momentum Amplitude: π_{nma} ; T_{start} : Start iteration; T_b : Weight updating cycle; Loss \leftarrow Compute using Equation.11

Output: self-adaptive weights \mathcal{W}_m^t and \mathcal{W}_I^t

```

1: while train do
2:   if  $t \leq T_{start}$  then
3:     Initialise  $\mathcal{W}_m^0 \leftarrow 0.8$  and  $\mathcal{W}_I^0 \leftarrow 0.2$ 
4:     Initialise  $L_m$  using Equation.3
5:   else
6:     Update  $L_m$  using Equation.3
7:     if  $t \% T_b == 0$  then
8:       Compute  $\Delta l$  using  $L_m$  and Equation.4
9:       Compute  $\Delta w$  using  $\Delta l$  and Equation.5
10:      Update  $\mathcal{W}_m^t$  and  $\mathcal{W}_I^t$  using Equation.6
11:   end if
12:   end if
13: end while

```

3.3. Exploration of Decoupled Decoding Structure

Detection transformer [2, 3, 7, 21, 27, 38] leverages the object queries to detect object instances, where each object query represents an object instance. In the decoding stage, the object queries are updated to query embeddings by connecting object queries with semantic information from the encoded semantic features. The generated query embeddings couple the location and category information for both object localization and identification process simultaneously. For open-world object detection, the model requires to detect the known objects, localize the unknown objects and identify them as the unknown class. For the parallel decoding structure, we observe that the inclusion of detecting unknown reduces the model's ability to detect known objects. Inspired by how humans subconsciously confront new scenarios, we propose to decouple the decoding process of DETR for mitigating the impact of unknown object detection on detecting known objects. In this paper, we explore two decoupled decoding ways, *i.e.*, the fully decoupled decoding structure and the cascade decoupled decoding structure.

3.3.1 Fully Decoupled Decoding Structure

For decoupling the location and category information, an intuitive way is to carry out the localization and identification process independently. Motivated by this, the fully decoupled decoding structure (FD) is proposed. In the fully decoupled decoding structure, location and class queries are two sets of mutually independent queries sent to the shared decoder. This operation of FD is shown in Figure 3 (a),

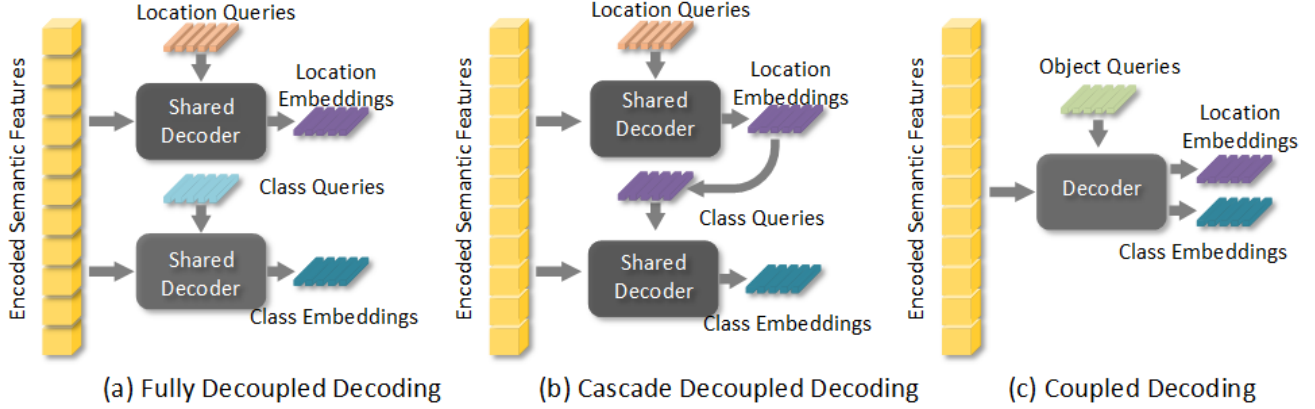


Figure 3. (a) The fully decoupled decoding structure has two independent decoding processes for localization and identification. (b) In the cascade decoupled decoding structure, the location embeddings are used as class queries for knowledge retention. (c) For the coupled decoding structure, the same query is put into the decoder for localization and identification.

which is formulated as follows:

$$\mathcal{E}_{\text{Location}} = \mathcal{F}_s(\mathcal{F}_e(\mathcal{O}(\mathcal{J}), P_n), P_m, Q_{\text{Location}}, \mathcal{R}), \quad (7)$$

$$\mathcal{E}_{\text{Class}} = \mathcal{F}_s(\mathcal{F}_e(\mathcal{O}(\mathcal{J}), P_n), P_m, Q_{\text{Class}}, \mathcal{R}), \quad (8)$$

where $\mathcal{F}_s(\cdot)$ denotes the shared decoder. $\mathcal{F}_e(\cdot)$ is the encoder and $\mathcal{O}(\cdot)$ is the backbone. P_n and P_m stands for the positional encoding and embeddings, respectively. \mathcal{R} represents the reference points and \mathcal{J} denotes the input image. Q_{Class} stands for the class queries.

3.3.2 Cascade Decoupled Decoding Structure

Inspired by how people react to new scenarios, a cascade decoupled decoding structure is proposed to decode the encoded features in a cascade way so that the localization process is not restricted by the category information, while the identification process can get help from the location knowledge in the cascade structure. The operation of localization and identification cascade decoding structure is expressed as follows:

$$\mathcal{E}_{\text{Location}} = \mathcal{F}_s(\mathcal{F}_e(\mathcal{O}(\mathcal{J}), P_n), P_m, Q_{\text{Location}}, \mathcal{R}), \quad (9)$$

$$\mathcal{E}_{\text{Class}} = \mathcal{F}_s(\mathcal{F}_e(\mathcal{O}(\mathcal{J}), P_n), P_m, \mathcal{E}_{\text{Location}}, \mathcal{R}). \quad (10)$$

As shown in Figure 3 (b), the location embeddings are used as class queries to generate class embeddings.

3.4. Training and Inference

Our CAT is trained end-to-end using the following joint loss formulation:

$$L = L_{\text{localization}} + L_{\text{identification}} + L_{\text{objectness}}, \quad (11)$$

where $L_{\text{localization}}$, $L_{\text{identification}}$ and $L_{\text{objectness}}$ denotes the loss terms for foreground localization, novelty

identification and object scoring, respectively. When a set of new categories are introduced at each episode, we employ an exemplar replay based finetuning to alleviate catastrophic forgetting of learned classes and then finetune the model using a balanced set of exemplars stored for each known class. The bounding boxes and categories predictions of the known and *top-k* unknown objects are simultaneous used during evaluation.

4. Experiments

4.1. Datasets and Metrics

The experiments are implemented on two mainstream splits of MS-COCO [23] and Pascal VOC [10] dataset. We group the classes into a set of nonoverlapping tasks $\{T^1, \dots, T^t, \dots\}$. The class in task T^c only appears in tasks where $t \geq c$. In task T^c , classes encountered in $\{T^c : c \leq t\}$ and $\{T^c : c > t\}$ are considered as known and unknown classes, respectively.

OWOD SPLIT [17] splits the 80 classes of MS-COCO into 4 tasks and selects training set for each task from the MS-COCO and Pascal VOC training set images. Pascal VOC testing and MS-COCO validation set are used for evaluation. See more details in Appendix A.2.

MS-COCO SPLIT [13] mitigates data leakage across tasks in [17] and is more challenging. The training and testing data are selected from MS-COCO.

Metrics: Following the most commonly used evaluation metric for object detection, we use mean average precision (mAP) to evaluate the known objects. Inspired by [1, 9, 13, 17, 25], U-Recall, Wilderness Impact (WI, see detailed in Appendix A.3) and Absolute Open-Set Error (AOSE) are used as main metric for unknown objects. U-Recall measures the ability of the model to retrieve un-

Table 1. State-of-the-art comparison on OWOD split. The comparison is shown in terms of U-Recall, WI, A-OSE and known class mAP. U-Recall measures the ability of the model to retrieve unknown object instances for OWOD problem. Both WI and A-OSE implicitly quantify the effectiveness of the model in handling unknown objects. For a fair comparison, we compare with the recently introduced OW-DETR [13] and ORE [17] not employing EBUI (the results are reproduced by the same GPUs as our model). The CAT achieves improved all metrics over the existing works across all tasks, demonstrating our model’s effectiveness for OWOD problem. U-Recall, WI and A-OSE cannot be computed in Task 4 due to the absence of unknown test annotations, for the reason that all 80 classes are known.

Task IDs →	Task 1				Task 2						Task 3						Task 4		
	U-Recall	WI	A-OSE	mAP(↑)	U-Recall	WI	A-OSE	mAP(↑)			U-Recall	WI	A-OSE	mAP(↑)			mAP(↑)		
	(↑)	(↓)	(↓)	Current known	(↑)	(↓)	(↓)	Previously known	Current known	Both	(↑)	(↓)	(↓)	Previously known	Current known	Both	Previously known	Current known	Both
Faster-RCNN [33]	-	0.0699	13396	56.4	-	0.0371	12291	3.7	26.7	15.2	-	0.0213	9174	2.5	15.2	6.7	0.8	14.5	4.2
Faster-RCNN + Finetuning	Not applicable in Task 1				-	0.0375	12497	51.0	25.0	38.0	-	0.0279	9622	38.2	13.6	30.0	29.7	13.0	25.6
DETR [38]	-	0.0608	33270	60.3	-	0.0368	18115	4.5	31.3	17.9	-	0.0197	9392	3.3	22.5	8.5	2.5	16.4	6.0
DETR + Finetuning	Not applicable in Task 1				-	0.0337	17834	54.5	34.4	44.8	-	0.0195	10095	40.0	17.8	33.3	32.5	20.0	29.4
Cascade	-	0.0476	42083	60.5	-	0.0308	21928	5.0	33.7	19.2	-	0.0189	12189	4.2	24.9	10.2	3.6	18.2	7.6
Cascade + Finetuning	Not applicable in Task 1				-	0.0296	20587	55.4	35.0	46.0	-	0.0184	12854	42.4	19.2	35.2	34.6	21.8	31.6
ORE-EBUI [17]	4.9	0.0621	10459	56.0	2.9	0.0282	10445	52.7	26.0	39.4	3.9	0.0211	7990	38.2	12.7	29.7	29.6	12.4	25.3
OW-DETR [13]	7.1	0.0590	10248	58.9	6.8	0.0279	8540	52.9	29.1	41.0	7.8	0.0191	6840	38.1	14.7	30.3	30.8	13.3	26.4
Ours:CAT	21.8 (+14.7)	0.0581 (-0.0009)	7070 (-3178)	59.9 (+1.0)	18.6 (+11.8)	0.0263 (-0.0016)	5902 (-2638)	54.0 (+1.1)	33.6 (+4.5)	43.8 (+2.8)	23.9 (+16.1)	0.0177 (-0.0014)	5189 (-1651)	42.1 (+4.0)	19.8 (+5.1)	34.7 (+4.4)	35.1 (+4.3)	17.1 (+3.8)	30.6 (+4.2)

Table 2. State-of-the-art comparison on MS-COCO split. The comparison is shown in terms of U-Recall and mAP. Although the MS-COCO split is more challenging, our model gets a more significant improvement on this in comparison to ORE and OW-DETR. The significant metric improvements demonstrate that our CAT has the ability to retrieve new knowledge beyond the range of closed set and would not be limited by category knowledge of existing objects. See Sec.4.3 for more details.

Task IDs ↓	Metrics		ORE	OW-DETR	Ours:CAT
Task1	U-Recall(↑)		1.5	5.7	24.0 (+18.3)
	mAP(↑)	Current known	61.4	71.5	74.2 (+2.7)
Task2	U-Recall(↑)		3.9	6.2	23.0 (+16.8)
	mAP(↑)	Previously known	56.5	62.8	67.6 (+4.8)
		Current known	26.1	27.5	35.5 (+8.0)
		Both	40.6	43.8	50.7 (+6.9)
Task3	U-Recall(↑)		3.6	6.9	24.6 (+17.7)
	mAP(↑)	Previously known	38.7	45.2	51.2 (+6.0)
		Current known	23.7	24.9	32.6 (+7.7)
		Both	33.7	38.5	45.0 (+6.5)
Task4	mAP(↑)	Previously known	33.6	38.2	45.4 (+7.2)
		Current known	26.3	28.1	35.1 (+7.0)
		Both	31.8	33.1	42.8 (+9.7)

known object instances for OWOD problem. Both WI and A-OSE implicitly quantify the effectiveness of the model in handling unknown objects.

4.2. Implementation Details

The multi-scale feature extractor consists of a Resnet-50 [16] pretrained on ImageNet [8] in a self-supervised [4] manner and a deformable transformer encoder whose number of layer is set to 6. For the shared decoder, we use a

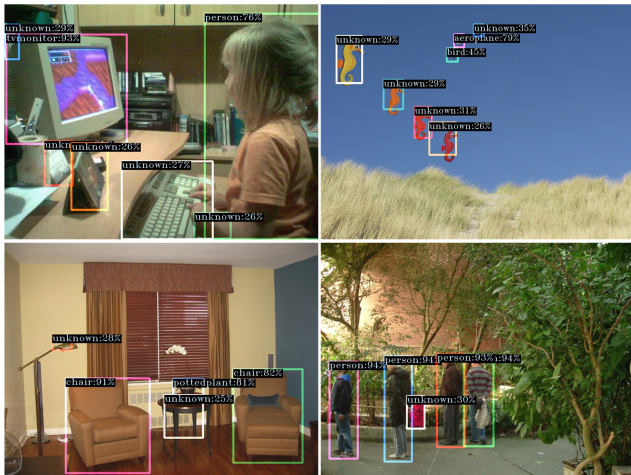
deformable transformer decoder and the number of layer is set to 6, too. We set the number of queries $M = 100$, the dimension of the embeddings $D = 256$ and the number of pseudo-labels $k = 5$. During inference, *top-50* high scoring detections are used for evaluation for per image. More details are described in the Appendix A.4.

4.3. Comparison With State-of-the-art Methods

For a fair comparison, we compare CAT with ORE [17] without the energy-based unknown identifier (EBUI) that relies on held-out validation data with weak unknown object supervision and OW-DETR [13] to demonstrate the effectiveness of our method for OWOD problem. We present the comparison in terms of known class mAP, unknown class recall, WI, and A-OSE, where U-Recall, WI and A-OSE cannot be computed in Task 4 due to the absence of unknown test annotations, for the reason that all 80 classes are known. Furthermore, we demonstrate the effectiveness of our model for incremental object detection in comparison to [13, 17, 30, 35].

OWOD SPLIT: The results compared with the state-of-the-art methods on OWOD split for OWOD problem are shown in Table.1. The performance of proposed standard cascade detection transformer is also reported to be compared with Faster R-CNN [33] and the standard Deformable DETR [38] frameworks, for demonstrating the power of localization identification cascade structure. These three can only identify known objects, and so U-Recall cannot be computed for them. Benefiting from the self-adaptive pseudo-labelling, the ability of CAT to detect unknown objects goes substantially beyond the existing models. Compared with OW-DETR’s U-Recall of 7.1, 6.8 and 7.8 on Task 1, 2 and 3, our CAT achieves 21.8, 18.6 and 23.9 in the

corresponding tasks, achieving significant absolute gains up to 16.1%. In terms of WI and A-OSE, CAT also exceeds them in all tasks. The ability to detect known objects and alleviate catastrophic forgetting of previous knowledge gains an improved performance with significant gains, achieving significant absolute gains up to 4.4%. This demonstrates the significant performance of the cascade decoding structure. In addition, we report qualitative results in Figure 4, along with failure case analysis. See more detailed qualitative results in Appendix B.2.



Incremental Object Detection: To intuitively present our CAT’s ability for detecting object instances, we compare it to [13, 17, 30, 35] on the incremental object detection (IOD) task. We evaluate the experiments on three standard settings, where a group of classes (10, 5 and last class) are introduced incrementally to a detector trained on the remain-

ing classes (10, 15 and 19), based on PASCAL VOC 2007 dataset [10]. As the results shown in Table.3, CAT outperforms the existing method in a great migration on all three settings, indicating the power of localization and identification cascade detection transformer for IOD.

Table 3. State-of-the-art comparison for incremental object detection for three different settings on PASCAL VOC dataset. The comparison is shown in terms of overall mAP. Our CAT achieves significant performance in comparison to existing works on all the three settings. See more details in Sec.4.3 and Appendix B.1.

Method	10+10 settings	15+5 settings	19+1 settings
ILOD [35]	63.2	65.8	68.2
Faster ILOD [30]	62.1	67.9	68.5
ORE [17]	64.5	68.5	68.8
OW-DETR [13]	65.7	69.4	70.2
Ours: CAT	67.7 (+2.0)	72.2 (+2.8)	73.8 (+3.6)

4.4. Ablation Study

We conduct abundant ablative experiments to verify the effectiveness of CAT’s components on the OWO split [17].

Cascade Decoupled Decoding Structure: We compare between OW-DETR, fully decoupled decoding structure and CAT in Table.4. The results illustrate that the decoupled decoding structure improves the performance of detecting known objects and does mitigate the influence of unknown objects on the detection of known objects to some extent. Because it reduces the difficulty of parameter learning and mitigates the risk of confusion for known and unknown objects by disassembling the localization and identification process of detection. Compared with the fully decoupled decoding structure, the cascade decoupled decoding structure is able to allow the identification process to draw on location information while the localization process is not limited by category knowledge and outperforms it.

Self-Adaptive Pseudo-labelling: As shown in Figure.5 (a) and (b), we performed a number of ablation experiments on Task 1 for different update cycles, positive and negative momentum amplitudes. The results demonstrate that the self-adaptive pseudo-labelling makes the training process of CAT robust, as we analyzed earlier. Especially for the pink line, even if there are unexpected situations in the training process, CAT can still self-adjust and develop in a good direction. In addition, we compare the attention-driven (AD) and self-adaptive (SA) pseudo-labelling mechanism in Table.5 and Figure.5 (c). The results demonstrate that our self-adaptive pseudo-labelling mechanism significantly improves the model’s ability to retrieve unknown objects. During training, CAT requires double decoding processes so that it is affected by generated pseudo-labels twice as often as OW-DETR. Thus, for the high quality pseudo-

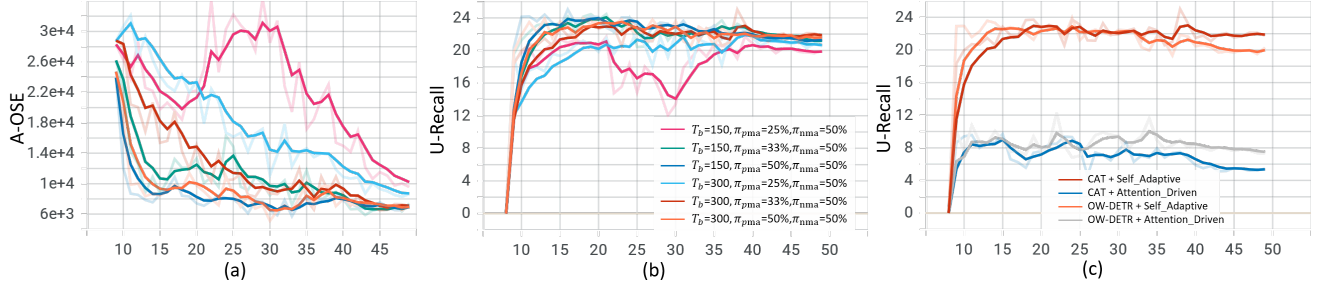


Figure 5. (a) and (b) illustrate performance comparison between different update cycles, positive and negative momentum amplitude on A-OSE and U-Recall. Where the cycle is set to 150 and 300, the positive momentum amplitude is set to 25%, 33% and 50%, the negative momentum amplitude is set to 50%, respectively. The lighter coloured lines are the real data and the corresponding darker coloured lines are the data after smoothing. (c) shows performance comparison between AD and SA. See detail in Sec.4.4.

Table 4. Performance comparison between different decoupled decoding structures and OW-DETR. ‘FD’ refers to the fully decoupled decoding structure. See more details in Sec.4.4.

Task IDs ↓	Metrics		OW-DETR	FD	CAT
Task1	mAP(↑)	Current known	59.3	57.9	59.9
Task2	mAP(↑)	Previously known	53.0	49.5	54.0
		Current known	29.4	29.4	33.6
		Both	41.3	39.4	43.8
Task3	mAP(↑)	Previously known	38.1	41.2	42.1
		Current known	15.0	18.5	19.8
		Both	30.5	33.5	34.7
Task4	mAP(↑)	Previously known	30.6	33.3	35.1
		Current known	14.0	15.8	17.1
		Both	26.8	28.9	30.6

labels, CAT could learn better to detect unknown objects than OW-DETR. For the low quality pseudo-labels, CAT would also be affected to a greater extent. The results in Table.5 further demonstrate this investigation and the robustness of our pseudo-labelling mechanism to generate pseudo labels.

Open-set Detection Comparison: To further demonstrate CAT’s ability to handle unknown instances in open-set data, we follow the same evaluation protocol as [13, 17, 26] and report the performance in Table.6. CAT achieves promising performance in comparison to the existing methods.

5. Relation to Prior Works

The issue of standard object detection [3, 6, 12, 15, 22, 24, 29, 32, 33, 38, 40] has been raised for several years, numerous works have investigated this problem and push the field to certain heights. Whereas the strong assumption that the label space of object categories to be encountered during the life-span of the model is the same as during its training results that these methods cannot meet real-world needs. The success of [11, 18–20, 28, 33] demonstrates the feasibility of

Table 5. Performance comparison AD and SA pseudo-labelling mechanism. The results demonstrate that SA substantially enhances the model’s ability to retrieve unknown objects

Method	Task IDs ↓	AD	SA	U-Recall	WI	A-OSE
OW-DETR	Task1	✓	✗	7.1	0.0590	10248
		✗	✓	19.8	0.0578	8360
	Task2	✓	✗	6.8	0.0279	8540
		✗	✓	16.8	0.0268	6452
	Task3	✓	✗	7.8	0.0191	6840
		✗	✓	21.8	0.0175	5310
CAT	Task1	✓	✗	5.4	0.0533	41474
		✗	✓	21.8	0.0581	7070
	Task2	✓	✗	4.9	0.0271	20410
		✗	✓	18.6	0.0263	5902
	Task3	✓	✗	6.0	0.0186	11078
		✗	✓	23.9	0.0177	5189

Table 6. Performance comparison on open-set object detection task. Our CAT achieves significant performance in comparison to existing works. See more details in Sec.4.4.

Evaluated on →	VOC	WR1
Standard Faster R-CNN [35]	81.8	77.1
Standard RetinaNet	79.2	73.8
Dropout Sampling [26]	78.1	71.1
ORE [17]	81.3	78.2
OW-DETR [13]	82.1	78.6
Ours: CAT	83.2 (+1.1)	79.5 (+0.9)

foreground localization based on the position and appearance of objects. ORE [17] and OW-DETR [13] leverage the models of standard object detection and pseudo labels to detect objects in open world. In this paper, we propose a novel transformer [37] based framework, CAT, for OWOD. CAT decouples the localization and identification process and connects them in a cascade approach. In CAT, the foreground localization process is not limited by the category

of known objects, whereas the process of foreground identification can use information from the localization process. Along with self-adaptive pseudo-labelling, CAT can gain information beyond the data annotation and maintain a stable learning process according to self-regulation.

6. Conclusions

In this paper, we analyze the drawbacks of the parallel decoding structure for open-world object detection and explore the decoupled decoding structures of the detection transformer. Motivated by the subconscious reactions of humans when facing new scenes, we propose a novel localization and identification cascade detection transformer (CAT), which decouples the localization and identification process via the cascade decoding structure. The cascade decoding structure alleviates the influence of detecting unknown objects on the detection of known objects. With the self-adaptive pseudo-labelling mechanism, CAT gains knowledge beyond the data annotation, generates pseudo labels with robustness and maintains a stable training process via self-adjustment. The extensive experiments on two popular benchmarks, *i.e.*, PASCAL VOC and MS COCO demonstrate that CAT consistently outperforms the existing works for all task settings on all splits and achieves state-of-the-art performance in the incremental object detection and open-set detection.

Acknowledgment

This work is supported by National Natural Science Foundation of China (grant No.61871106 and No.61370152), Key R&D projects of Liaoning Province, China (grant No.2020JH2/10100029), and the Open Project Program Foundation of the Key Laboratory of Opto-Electronics Information Processing, Chinese Academy of Sciences (OEIP-O-202002).

A. Additional Experiments Material

A.1. Theory For Self-Adaptive Pseudo-labelling

For $0 < w_2 < w_1 < 1$, we find the potential relationship as follows:

$$\begin{cases} x^{w_1} > x^{w_2}, & \text{if } x > 1 \\ x^{w_1} < x^{w_2}, & \text{if } x < 1 \end{cases} \quad (12)$$

Thus, for $x^{w_1} \cdot y^{w_2}$ and $w_1 > w_2$, if $x > 1$ and $y > 1$, x weights more and y weights more if $x < 1$ and $y < 1$.

For the self-adaptive pseudo-labelling, we first normalize s_o to the range 0 to 1. Considering that the model itself has little knowledge in the early stages of model training, the model-driven pseudo-labelling should weight less than the input-deiven pseudo-labelling. As the training time of the model increasing, the knowledge base of the model grows and the weight of the model-driven pseudo-labelling

gets bigger. Combining this with the patterns above, we set \mathcal{W}_m^0 to 0.8, \mathcal{W}_l^0 to 0.2 and update them as follows:

$$\begin{cases} \mathcal{W}_m^t = \mathcal{W}_m^{t-1} + \Delta w \times \mathcal{W}_m^{t-1}, \\ \mathcal{W}_l^t = \mathcal{W}_l^{t-1} - \Delta w \times \mathcal{W}_l^{t-1}, \\ \mathcal{W}_m^t, \mathcal{W}_l^t = \text{norm}(\mathcal{W}_m^t, \mathcal{W}_l^t), \end{cases} \quad (13)$$

A.2. Additional Illustration For Data Split

As shown in Table.7, the OWOD split proposed in ORE groups all VOC classes and data as *Task 1*. The remaining 60 classes of MS-COCO are grouped into three successive tasks (*Task 2, 3, 4*) with semantic drifts. However, it leads data leakage across tasks since different classes which belong to a super-categories are introduced in different tasks. The MS-COCO split proposed in OW-DETR is a stricter split, where all the classes of a super-categories are introduced at a time in a task.

Table 7. The table shows task composition in the OWOD and MS-COCO split for Open-world evaluation protocol. The semantics of each task and the number of images and instances(objects) across splits are shown.

Task ID	Task 1	Task 2	Task 3	Task 4
OWOD split				
Semantic split	VOC Classes	Outdoor, Accessories, Appliances, Truck	Sports, Food	Electronic, Indoor, Kitchen, Furniture
# training images	16551	45520	39402	40260
# test images	4952	1914	1642	1738
# train instances	47223	113741	114452	138996
# test instances	14976	4966	4826	6039
MS-COCO split				
Semantic split	Animals, Person, Vehicles	Appliances, Accessories, Outdoor, Furniture	Sports, Food	Electronic, Indoor, Kitchen
# training images	89490	55870	39402	38903
# test images	3793	2351	1642	1691
# train instances	421243	163512	114452	160794
# test instances	17786	7159	4826	7010

A.3. WI, A-OSE and U-Recall Metrics

In this paper, we mainly illustrate the state-of-the-art comparison in terms of wilderness impact (WI), absolute open-set error (A-OSE), unknown recall (U-Recall) and mean average precision (mAP). WI measures the model's confusion in predicting an unknown instance as known class. The calculation formula is as follows:

$$WI = \frac{P_{\mathcal{K}}}{P_{\mathcal{K} \cup \mathcal{U}}} - 1 \quad (14)$$

Where $P_{\mathcal{K}}$ is the prediction on known classes and $P_{\mathcal{K} \cup \mathcal{U}}$ is the prediction on known and unknown classes. A-OSE devotes the total number of unknown instances detected as known classes. Both WI and A-OSE indicate the degree of confusion in predicting the known classes in the presence

of unknown instances. Furthermore, U-Recall directly measures the model’s ability to retrieve the unknown instances.

A.4. Additional Implementation Details

For selective search, we use the *selective_search* function in Selectivesearch library and the scale, sigma, min_size of parameter is set to 500, 0.9 and 200, respectively. In addition, we eliminate candidate boxes with less than 2000 pixel points. The multi-scale feature maps extracted from the backbone are projected to feature maps with 256-channels using 1×1 convolution filters and used as multi-scale input to deformable transformer encoder. The PyTorch library and eight NVIDIA RTX 3090 GPUs are used to train our CAT framework with a batch size of 3 images per GPUs. In each task, the CAT framework is trained for 50 epochs and finetuned for 20 epochs during the incremental learning step. We train our CAT using the Adam optimizer with a base learning rate of 2×10^{-4} , $\beta_1 = 0.9$, $\beta_2 = 0.999$, and weight decay of 10^{-4} . For finetuning during incremental step, the learning rate is reduced by a factor of 10 and trained using a set of 50 stored exemplars per known class.

B. Additional Results

B.1. Incremental Object Detection

Table.8 shows a detailed comparison of CAT with existing approaches on PASCAL VOC. Evaluation is performed on three standard settings, where a group of classes (10, 5 and last class) are introduced incrementally to a detector trained on the remaining classes (10,15 and 19). Our CAT performs favorably against existing approaches on all three settings, illustrating the power of localization identification cascade detection transformer for incremental objection detection.

B.2. Additional Qualitative Results

Figure.6 illustrates the visualization results comparison between OW-DETR and our CAT. We use OW-DETR and CAT which are both trained on Task 1, the known classes are ‘aeroplane’, ‘bicycle’, ‘bird’, ‘boat’, ‘bottle’, ‘bus’, ‘car’, ‘cat’, ‘chair’, ‘cow’, ‘diningtable’, ‘dog’, ‘horse’, ‘motorbike’, ‘person’, ‘pottedplant’, ‘sheep’, ‘sofa’, ‘train’ and ‘tvmonitor’. The results show that our CAT substantially outperforms OW-DETR in terms of the ability to explore unknown objects and the accuracy of detection due to the clever cascade decoupled decoding structure and self-adaptive pseudo-labelling. As shown in the first row, OW-DETR identifies the background and known objects as unknowns and the real unknown object (*carton*) as the background, and our model accurately identifies the *carton* as the unknown object. In the second row, OW-DETR iden-

tifies the two *calendars* as the *chair* and the background, respectively, and the *keyboard* as the background, and our CAT accurately identifies them as unknown objects. The third row shows that OW-DETR fails to detect the true unknown object (*frame*) and identifies two known objects (*sofa*) as one. Our model accurately identifies the *frame* as an unknown object and also accurately identifies the two *sofas*.

Figure.7 describes the visualization results comparison between CAT and Oracle. We visualize the detection results of our model for known and unknown objects, as well as the ground truth on the tasks corresponding to the weights, including the labels of known and unknown categories, where the objects of unknown categories are the objects of other categories that have not yet appeared in the total categories of the dataset. Our model can accurately detect known objects and unknown objects outside the total class of the dataset, such as the *electric plug* and *sound switch* in the first row, the *camera* in the second row and the *kitten toy* in the third row. It is also worth noting that although our model detects the *audio*, it does not identify it as an unknown object, but as a *remote*, showing the limitations of our model.

Figure.8 exhibits the visualization performance on incremental object detection. We visualize the detection results of the weights corresponding to different tasks for the same scenario. The results show that our CAT can identify unknown kinds of objects as the unknown class and accurately identify their classes after incrementally learning the unknown classes, such as *sports ball* and *tennis racket* in the first row, *surfboard* in the second row and *traffic light* in the third row.

C. Societal Impact and Limitations

Open-world object detection makes artificial intelligence smarter to face more problems in real life. It takes object detection to a cognitive level, as the model requires more than simply remembering the objects learned, it requires deeper thinking about the scene.

Although our results demonstrate significant improvements over ORE and OW-DETR in terms of WI, A-OSE, U-Recall and mAP, the performances are still on the lower side due to the challenging nature of the open-world detection problem. In this paper, we are mainly committed to enhance the model’s ability to explore unknown classes. However, the confidence level of our model for the detection of unknown objects still needs to be improved, and this is what we will strive for in the future.

References

- [1] Ankan Bansal, Karan Sikka, Gaurav Sharma, Rama Chellappa, and Ajay Divakaran. Zero-shot object detection. In

OW-DETR

Ours:CAT

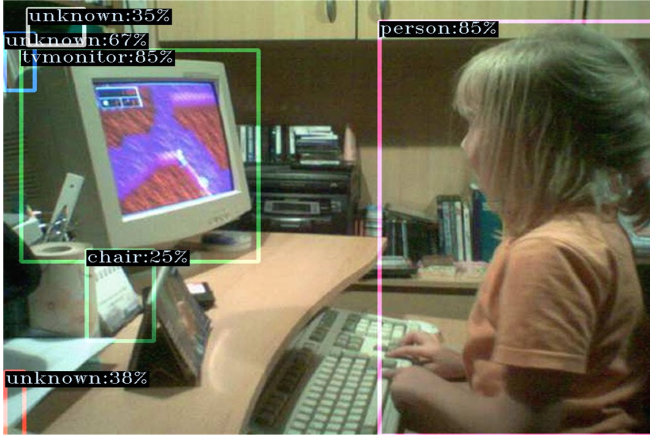
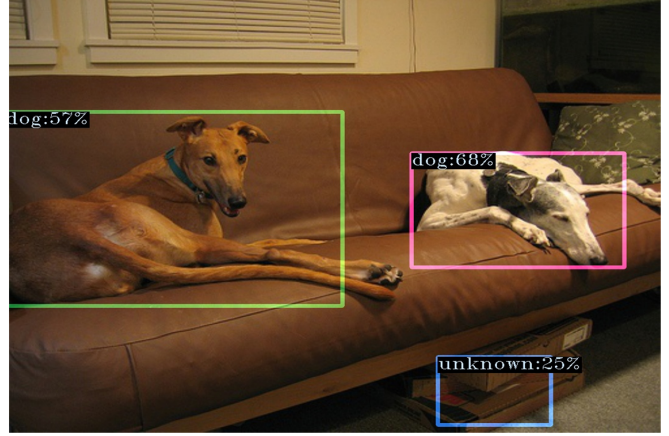
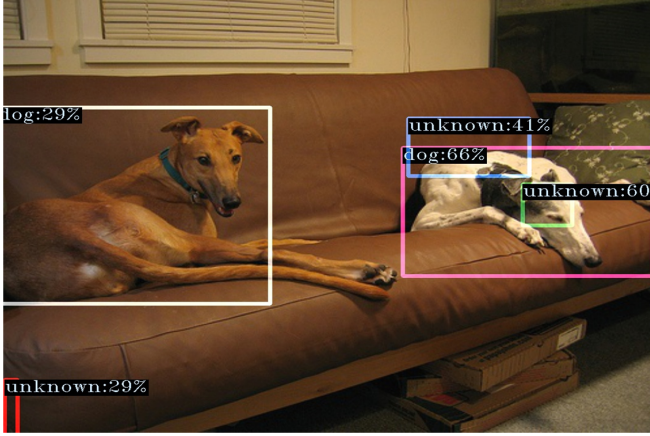


Figure 6. Visualization results comparison between OW-DETR and our CAT. We use OW-DETR and CAT which are both trained on Task 1, the known classes are ‘aeroplane’, ‘bicycle’, ‘bird’, ‘boat’, ‘bottle’, ‘bus’, ‘car’, ‘cat’, ‘chair’, ‘cow’, ‘diningtable’, ‘dog’, ‘horse’, ‘motorbike’, ‘person’, ‘pottedplant’, ‘sheep’, ‘sofa’, ‘train’ and ‘tvmonitor’. The results show that our CAT substantially outperforms OW-DETR in terms of the ability to explore unknown objects and the accuracy of detection due to the clever cascade decoupled decoding structure and self-adaptive pseudo-labelling mechanism. As shown in the first row, OW-DETR identifies the background and known objects as unknowns and the real unknown object (*carton*) as the background, and our model accurately identifies the *carton* as the unknown object. In the second row, OW-DETR identifies the two *calendars* as the *chair* and the background, respectively, and the *keyboard* as the background, and our CAT accurately identifies them as unknown objects. The third row shows that OW-DETR not only does not detect the true unknown object (*frame*), but also identifies two known objects (*sofa*) as one. Our model accurately identifies the frame as an unknown object and also accurately identifies the two *sofas*.

Table 8. The detailed comparison of CAT with existing approaches on PASCAL VOC. Evaluation is performed on three standard settings, where a group of classes (10, 5 and last class) are introduced incrementally to a detector trained on the remaining classes (10,15 and 19). Our CAT performs favorably against existing approaches on all three settings, illustrating the power of localization identification cascade detection transformer for incremental objection detection.

10 + 10 setting	aero	cycle	bird	boat	bottle	bus	car	cat	chair	cow	table	dog	horse	bike	person	plant	sheep	sofa	train	tv	mAP
ILOD	69.9	70.4	69.4	54.3	48	68.7	78.9	68.4	45.5	58.1	59.7	72.7	73.5	73.2	66.3	29.5	63.4	61.6	69.3	62.2	63.2
Faster ILOD	72.8	75.7	71.2	60.5	61.7	70.4	83.3	76.6	53.1	72.3	36.7	70.9	66.8	67.6	66.1	24.7	63.1	48.1	57.1	43.6	62.1
ORE - (CC + EBUI)	53.3	69.2	62.4	51.8	52.9	73.6	83.7	71.7	42.8	66.8	46.8	59.9	65.5	66.1	68.6	29.8	55.1	51.6	65.3	51.5	59.4
ORE - EBUI	63.5	70.9	58.9	42.9	34.1	76.2	80.7	76.3	34.1	66.1	56.1	70.4	80.2	72.3	81.8	42.7	71.6	68.1	77	67.7	64.5
OW - DETR	75.4	63.9	57.9	50.0	52.0	70.9	79.5	72.4	44.3	57.9	59.7	73.5	77.7	75.2	76.2	44.9	68.8	65.4	79.3	69.0	65.7
Ours: CAT	76.5	75.7	67.0	51.0	62.4	73.2	82.3	83.7	42.7	64.4	56.8	74.1	75.8	79.2	78.1	39.9	65.1	59.6	78.4	67.4	67.7
15 + 5 setting	aero	cycle	bird	boat	bottle	bus	car	cat	chair	cow	table	dog	horse	bike	person	plant	sheep	sofa	train	tv	mAP
ILOD	70.5	79.2	68.8	59.1	53.2	75.4	79.4	78.8	46.6	59.4	59	75.8	71.8	78.6	69.6	33.7	61.5	63.1	71.7	62.2	65.8
Faster ILOD	66.5	78.1	71.8	54.6	61.4	68.4	82.6	82.7	52.1	74.3	63.1	78.6	80.5	78.4	80.4	36.7	61.7	59.3	67.9	59.1	67.9
ORE - (CC + EBUI)	65.1	74.6	57.9	39.5	36.7	75.1	80	73.3	37.1	69.8	48.8	69	77.5	72.8	76.5	34.4	62.6	56.5	80.3	65.7	62.6
ORE - EBUI	75.4	81	67.1	51.9	55.7	77.2	85.6	81.7	46.1	76.2	55.4	76.7	86.2	78.5	82.1	32.8	63.6	54.7	77.7	64.6	68.5
OW - DETR	78.0	80.7	79.4	70.4	58.8	65.1	84.0	86.2	56.5	76.7	62.4	84.8	85.0	81.8	81.0	34.3	48.2	57.9	62.0	57.0	69.4
Ours: CAT	75.3	81.0	84.4	64.5	56.6	74.4	84.1	86.6	53.0	70.1	72.4	83.4	85.5	81.6	81.0	32.0	58.6	60.7	81.6	63.5	72.2
19 + 1 setting	aero	cycle	bird	boat	bottle	bus	car	cat	chair	cow	table	dog	horse	bike	person	plant	sheep	sofa	train	tv	mAP
ILOD	69.4	79.3	69.5	57.4	45.4	78.4	79.1	80.5	45.7	76.3	64.8	77.2	80.8	77.5	70.1	42.3	67.5	64.4	76.7	62.7	68.2
Faster ILOD	64.2	74.7	73.2	55.5	53.7	70.8	82.9	82.6	51.6	79.7	58.7	78.8	81.8	75.3	77.4	43.1	73.8	61.7	69.8	61.1	68.5
ORE - (CC + EBUI)	60.7	78.6	61.8	45	43.2	75.1	82.5	75.5	42.4	75.1	56.7	72.9	80.8	75.4	77.7	37.8	72.3	64.5	70.7	49.9	64.9
ORE - EBUI	67.3	76.8	60	48.4	58.8	81.1	86.5	75.8	41.5	79.6	54.6	72.8	85.9	81.7	82.4	44.8	75.8	68.2	75.7	60.1	68.8
OW - DETR	82.2	80.7	73.9	56.0	58.6	72.1	82.4	79.6	48.0	72.8	64.2	83.3	83.1	82.3	78.6	42.1	65.5	55.4	82.9	60.1	70.2
Ours: CAT	86.0	85.8	78.8	65.3	61.3	71.4	84.8	84.8	52.9	78.4	71.6	82.7	83.8	81.2	80.7	43.7	75.9	58.5	85.2	61.1	73.8

Proceedings of the European Conference on Computer Vision (ECCV), pages 384–400, 2018. 5

- [2] Josh Beal, Eric Kim, Eric Tzeng, Dong Huk Park, Andrew Zhai, and Dmitry Kislyuk. Toward transformer-based object detection. *arXiv preprint arXiv:2012.09958*, 2020. 4
- [3] Nicolas Carion, Francisco Massa, Gabriel Synnaeve, Nicolas Usunier, Alexander Kirillov, and Sergey Zagoruyko. End-to-end object detection with transformers. In *European conference on computer vision*, pages 213–229. Springer, 2020. 2, 4, 8
- [4] Mathilde Caron, Hugo Touvron, Ishan Misra, Hervé Jégou, Julien Mairal, Piotr Bojanowski, and Armand Joulin. Emerging properties in self-supervised vision transformers. In *Proceedings of the IEEE/CVF International Conference on Computer Vision*, pages 9650–9660, 2021. 6
- [5] Xinlei Chen, Haoqi Fan, Ross Girshick, and Kaiming He. Improved baselines with momentum contrastive learning. *arXiv preprint arXiv:2003.04297*, 2020. 4
- [6] Xingyu Chen, Junzhi Yu, Shihan Kong, Zhengxing Wu, and Li Wen. Joint anchor-feature refinement for real-time accurate object detection in images and videos. *IEEE Transactions on Circuits and Systems for Video Technology*, 31(2):594–607, 2020. 8
- [7] Xiyang Dai, Yinpeng Chen, Jianwei Yang, Pengchuan Zhang, Lu Yuan, and Lei Zhang. Dynamic detr: End-to-end object detection with dynamic attention. In *Proceedings of the IEEE/CVF International Conference on Computer Vision*, pages 2988–2997, 2021. 4
- [8] Jia Deng, Wei Dong, Richard Socher, Li-Jia Li, Kai Li, and Li Fei-Fei. Imagenet: A large-scale hierarchical image database. In *2009 IEEE conference on computer vision and pattern recognition*, pages 248–255. Ieee, 2009. 6
- [9] Akshay Dhamija, Manuel Gunther, Jonathan Ventura, and Terrance Boulton. The overlooked elephant of object detection: Open set. In *Proceedings of the IEEE/CVF Winter Conference on Applications of Computer Vision*, pages 1021–1030, 2020. 5
- [10] Mark Everingham, Luc Van Gool, Christopher KI Williams, John Winn, and Andrew Zisserman. The pascal visual object classes (voc) challenge. *International journal of computer vision*, 88(2):303–338, 2010. 5, 7
- [11] Spyros Gidaris and Nikos Komodakis. Attend refine repeat: Active box proposal generation via in-out localization. *arXiv preprint arXiv:1606.04446*, 2016. 8
- [12] Ross Girshick. Fast r-cnn. In *Proceedings of the IEEE international conference on computer vision*, pages 1440–1448, 2015. 8
- [13] Akshita Gupta, Sanath Narayan, KJ Joseph, Salman Khan, Fahad Shahbaz Khan, and Mubarak Shah. Ow-detr: Open-world detection transformer. In *CVPR*, 2022. 2, 3, 5, 6, 7, 8
- [14] Kaiming He, Haoqi Fan, Yuxin Wu, Saining Xie, and Ross Girshick. Momentum contrast for unsupervised visual representation learning. In *Proceedings of the IEEE/CVF conference on computer vision and pattern recognition*, pages 9729–9738, 2020. 4
- [15] Kaiming He, Georgia Gkioxari, Piotr Dollár, and Ross Girshick. Mask r-cnn. In *Proceedings of the IEEE international conference on computer vision*, pages 2961–2969, 2017. 8

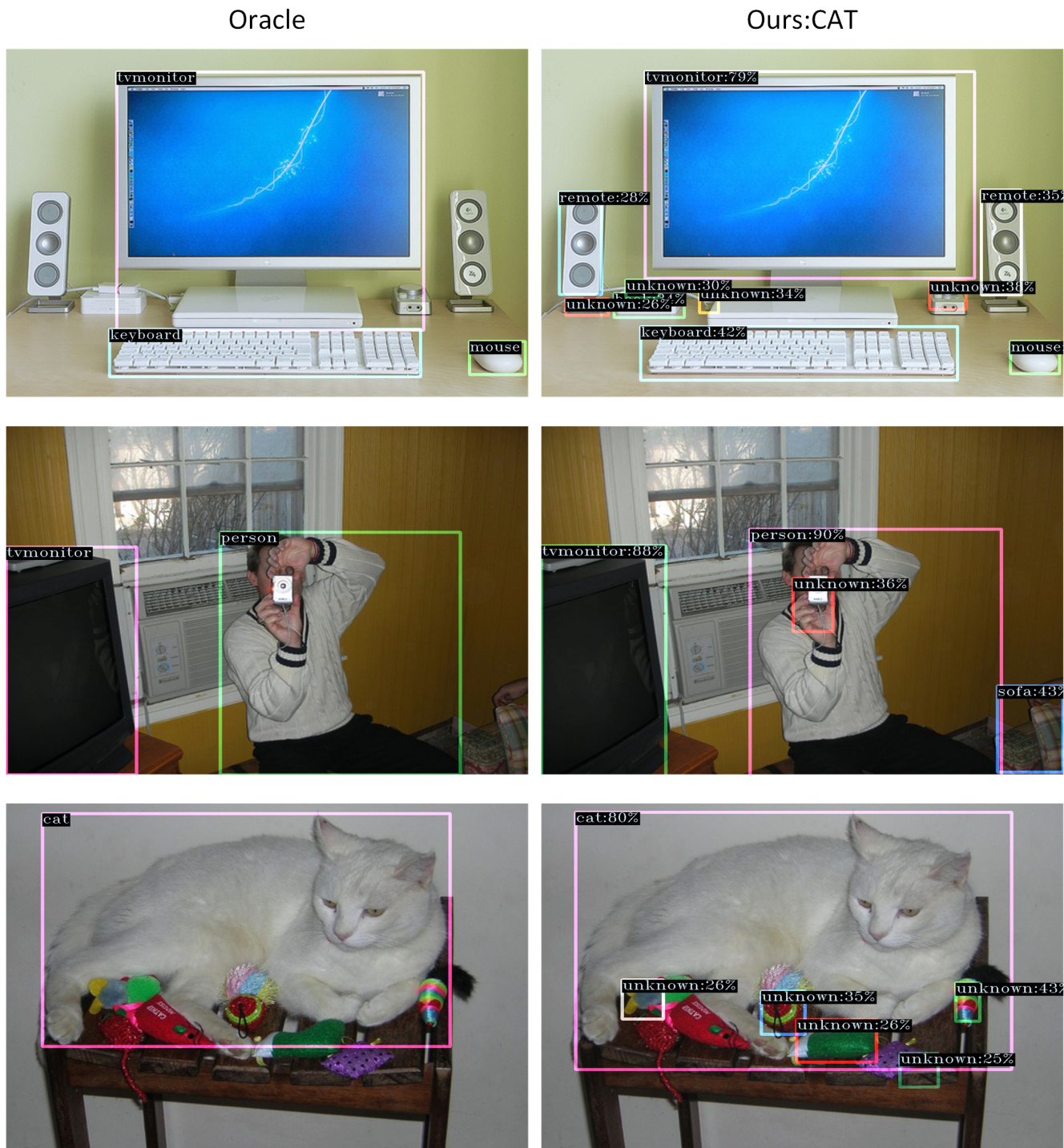


Figure 7. Visualization results comparison between CAT and Oracle. We visualize the detection results of our model for known and unknown objects, as well as the ground truth on the tasks corresponding to the weights, including the labels of known categories and the labels of unknown categories, where the objects of unknown categories are the objects of other categories that have not yet appeared in the total categories of the dataset. Our model can accurately detect known objects and unknown objects outside the total class of the dataset, such as the *electric plug* and *sound switch* in the first row, the *camera* in the second row and the *kitten toy* in the third row. It is also worth noting that although our model detects the *audio*, it does not identify it as an unknown object, but as a *remote*, showing the limitations of our model.

Before Learning

After Learning

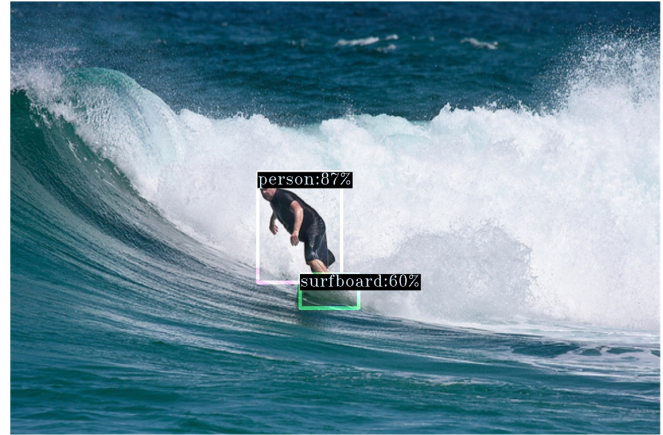
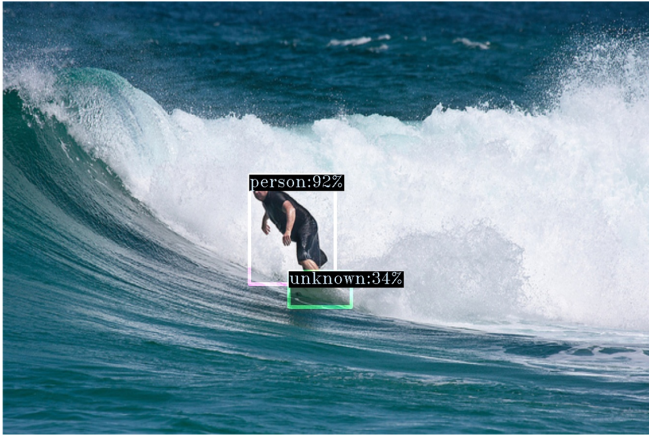


Figure 8. Visualization performance on incremental object detection. We visualize the detection results of the weights corresponding to different tasks for the same scenario. The results show that our CAT can identify unknown kinds of objects as the unknown class and accurately identify their classes after incrementally learning the unknown classes, such as *sports ball* and *tennis racket* in the first row, *surfboard* in the second row and *traffic light* in the third row.

[16] Kaiming He, Xiangyu Zhang, Shaoqing Ren, and Jian Sun.

Deep residual learning for image recognition. In *Proceed-*

- ings of the *IEEE conference on computer vision and pattern recognition*, pages 770–778, 2016. 6
- [17] K J Joseph, Salman Khan, Fahad Shahbaz Khan, and Vineeth N Balasubramanian. Towards open world object detection. In *2021 IEEE/CVF Conference on Computer Vision and Pattern Recognition (CVPR)*, pages 5826–5836, 2021. 1, 3, 4, 5, 6, 7, 8
 - [18] Bingyi Kang, Zhuang Liu, Xin Wang, Fisher Yu, Jiashi Feng, and Trevor Darrell. Few-shot object detection via feature reweighting. In *Proceedings of the IEEE/CVF International Conference on Computer Vision*, pages 8420–8429, 2019. 8
 - [19] Dahun Kim, Tsung-Yi Lin, Anelia Angelova, In So Kweon, and Weicheng Kuo. Learning open-world object proposals without learning to classify. *IEEE Robotics and Automation Letters*, 7(2):5453–5460, 2022. 8
 - [20] Hongyang Li, Yu Liu, Wanli Ouyang, and Xiaogang Wang. Zoom out-and-in network with map attention decision for region proposal and object detection. *International Journal of Computer Vision*, 127(3):225–238, 2019. 8
 - [21] Yanghao Li, Hanzi Mao, Ross Girshick, and Kaiming He. Exploring plain vision transformer backbones for object detection. *arXiv preprint arXiv:2203.16527*, 2022. 4
 - [22] Tsung-Yi Lin, Priya Goyal, Ross Girshick, Kaiming He, and Piotr Dollár. Focal loss for dense object detection. In *Proceedings of the IEEE international conference on computer vision*, pages 2980–2988, 2017. 8
 - [23] Tsung-Yi Lin, Michael Maire, Serge Belongie, James Hays, Pietro Perona, Deva Ramanan, Piotr Dollár, and C Lawrence Zitnick. Microsoft coco: Common objects in context. In *European conference on computer vision*, pages 740–755. Springer, 2014. 5
 - [24] Yue Lu, Xingyu Chen, Zhengxing Wu, and Junzhi Yu. Decoupled metric network for single-stage few-shot object detection. *IEEE Transactions on Cybernetics*, 2022. 8
 - [25] Dimity Miller, Lachlan Nicholson, Feras Dayoub, and Niko Sünderhauf. Dropout sampling for robust object detection in open-set conditions. In *2018 IEEE International Conference on Robotics and Automation (ICRA)*, pages 3243–3249. IEEE, 2018. 5
 - [26] Dimity Miller, Lachlan Nicholson, Feras Dayoub, and Niko Sünderhauf. Dropout sampling for robust object detection in open-set conditions. In *2018 IEEE International Conference on Robotics and Automation (ICRA)*, pages 3243–3249. IEEE, 2018. 8
 - [27] Ishan Misra, Rohit Girdhar, and Armand Joulin. An end-to-end transformer model for 3d object detection. In *Proceedings of the IEEE/CVF International Conference on Computer Vision*, pages 2906–2917, 2021. 4
 - [28] Pedro O O Pinheiro, Ronan Collobert, and Piotr Dollár. Learning to segment object candidates. *Advances in neural information processing systems*, 28, 2015. 8
 - [29] Yanwei Pang, Tiancai Wang, Rao Muhammad Anwer, Fahad Shahbaz Khan, and Ling Shao. Efficient featurized image pyramid network for single shot detector. In *Proceedings of the IEEE/CVF Conference on Computer Vision and Pattern Recognition*, pages 7336–7344, 2019. 8
 - [30] Can Peng, Kun Zhao, and Brian C Lovell. Faster ilod: Incremental learning for object detectors based on faster rcnn. *Pattern recognition letters*, 140:109–115, 2020. 6, 7
 - [31] Jordi Pont-Tuset, Pablo Arbeláez, Jonathan T. Barron, Ferran Marques, and Jitendra Malik. Multiscale combinatorial grouping for image segmentation and object proposal generation. *IEEE Transactions on Pattern Analysis and Machine Intelligence*, 39(1):128–140, 2017. 3
 - [32] Joseph Redmon, Santosh Divvala, Ross Girshick, and Ali Farhadi. You only look once: Unified, real-time object detection. In *Proceedings of the IEEE conference on computer vision and pattern recognition*, pages 779–788, 2016. 8
 - [33] Shaoqing Ren, Kaiming He, Ross Girshick, and Jian Sun. Faster r-cnn: Towards real-time object detection with region proposal networks. *Advances in neural information processing systems*, 28, 2015. 1, 6, 8
 - [34] Adrian Rosebrock. Intersection over union (iou) for object detection. *Diambil kembali dari PYImageSearch* <https://www.pyimagesearch.com/2016/11/07/intersection-over-union-iou-for-object-detection/>, 2016. 4
 - [35] Konstantin Shmelkov, Cordelia Schmid, and Karteek Alahari. Incremental learning of object detectors without catastrophic forgetting. In *Proceedings of the IEEE international conference on computer vision*, pages 3400–3409, 2017. 6, 7, 8
 - [36] Jasper RR Uijlings, Koen EA Van De Sande, Theo Gevers, and Arnold WM Smeulders. Selective search for object recognition. *International journal of computer vision*, 104(2):154–171, 2013. 3, 4
 - [37] Ashish Vaswani, Noam Shazeer, Niki Parmar, Jakob Uszkoreit, Llion Jones, Aidan N Gomez, Łukasz Kaiser, and Illia Polosukhin. Attention is all you need. *Advances in neural information processing systems*, 30, 2017. 8
 - [38] Xizhou Zhu, Weijie Su, Lewei Lu, Bin Li, Xiaogang Wang, and Jifeng Dai. Deformable detr: Deformable transformers for end-to-end object detection. *arXiv preprint arXiv:2010.04159*, 2020. 2, 4, 6, 8
 - [39] C Lawrence Zitnick and Piotr Dollár. Edge boxes: Locating object proposals from edges. In *European conference on computer vision*, pages 391–405. Springer, 2014. 3
 - [40] Zhengxia Zou, Zhenwei Shi, Yuhong Guo, and Jieping Ye. Object detection in 20 years: A survey. *arXiv preprint arXiv:1905.05055*, 2019. 8